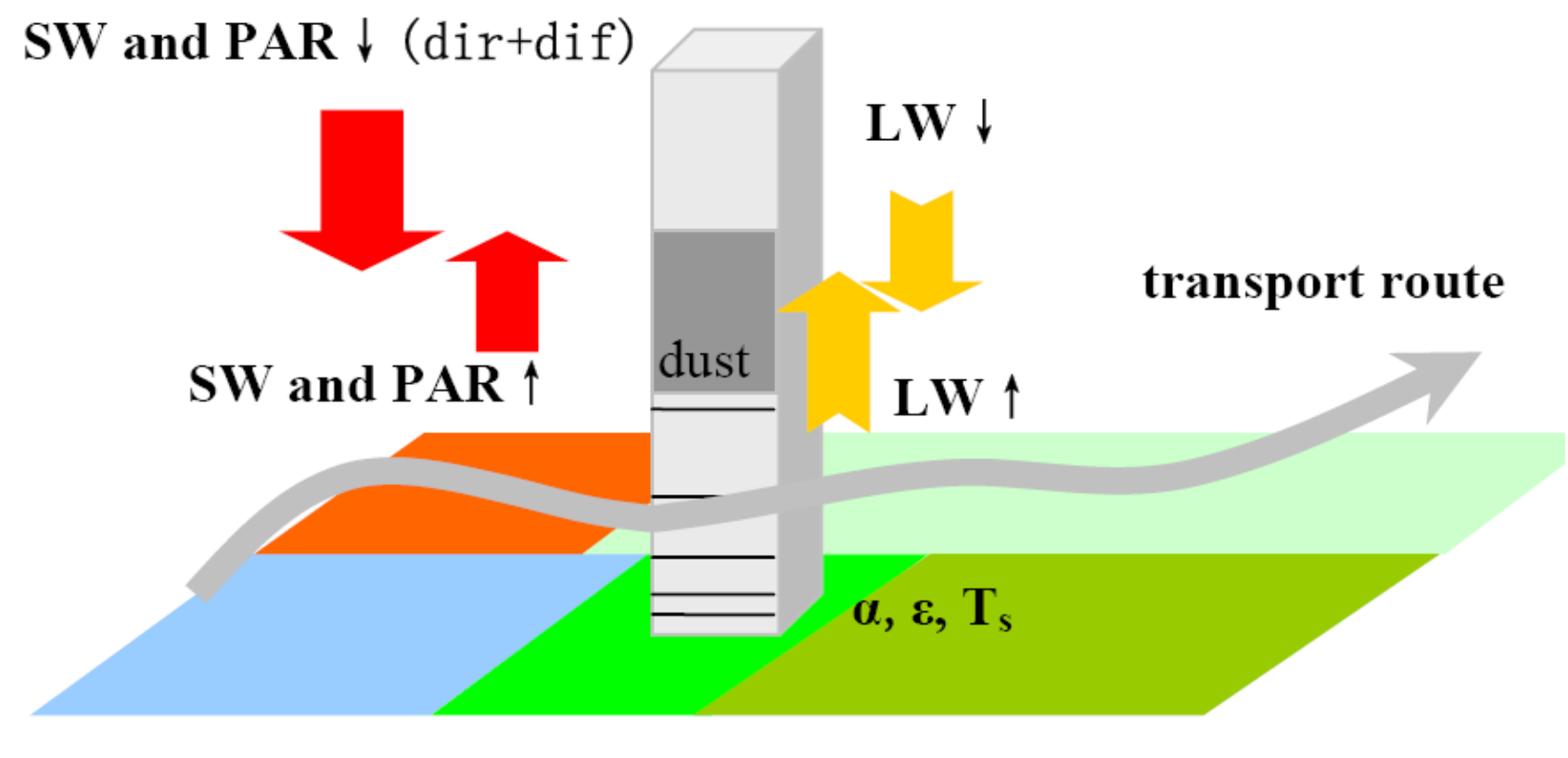
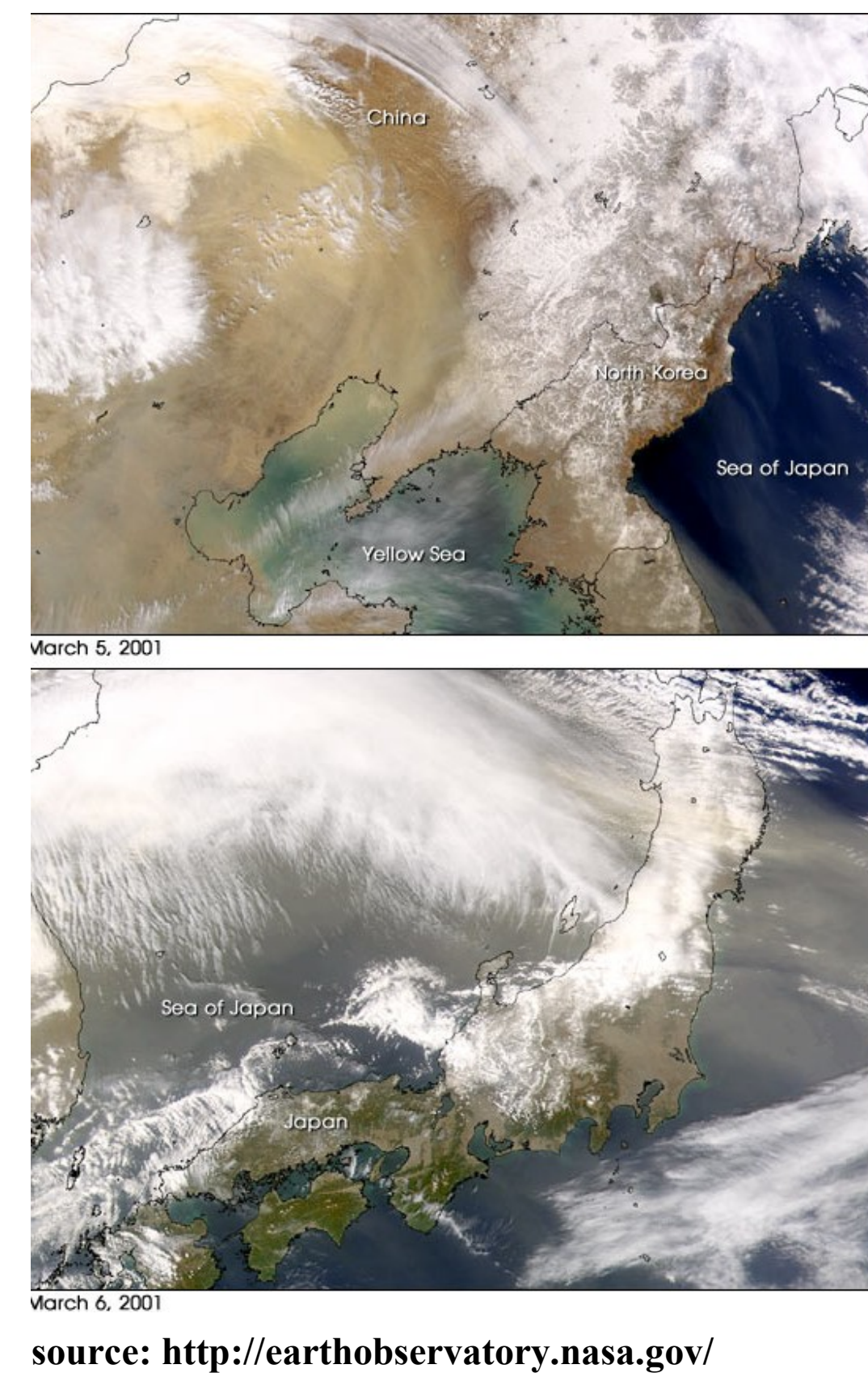
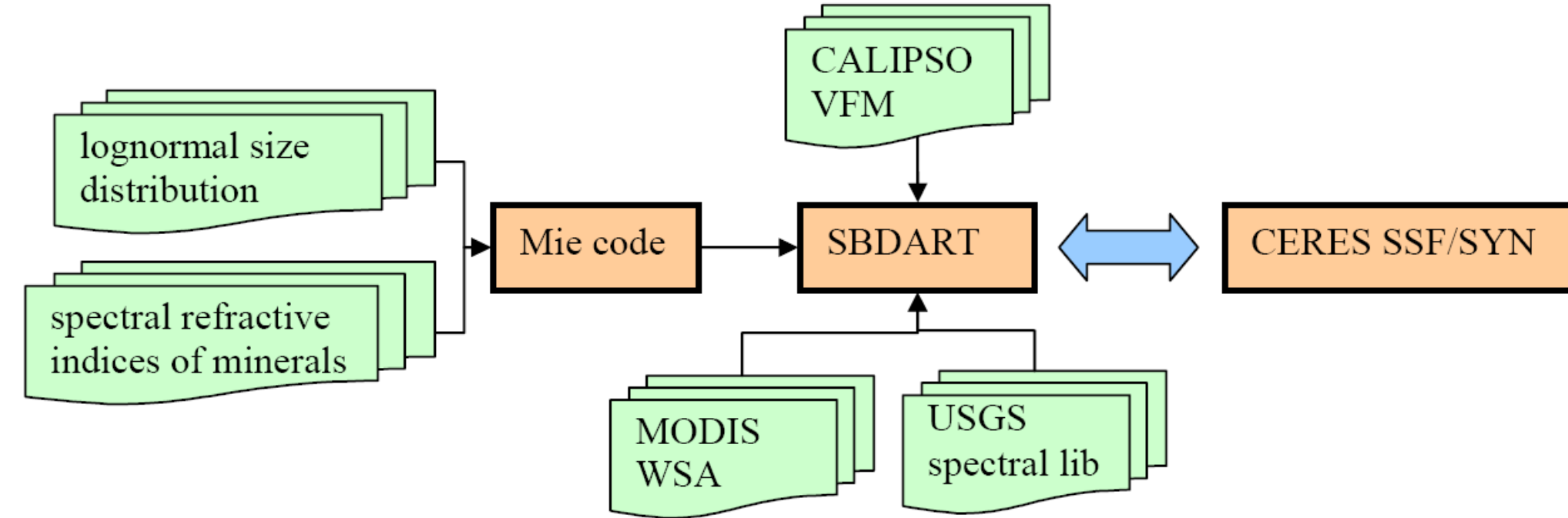


## 1. Motivation

- Aerosol impact on the shortwave (SW) and longwave (LW) components of surface energy balance and photosynthetically active radiation (PAR, 400–700 nm) is an important part of land ecosystem-atmosphere interactions.
- East Asia is an active source of wind-blown dust aerosol, especially in the spring season that is coincident with the onset of vegetation growth. Dust aerosol can be transported downwind affecting the terrestrial ecosystems over the large region.
- The goal of this study is to assess the range of the impact of mineral dust on PAR and surface radiative balance over the dryland ecosystems in East Asia by performing intensive 1D radiative transfer simulations considering the regional specifics of Asian dust properties and spectral surface albedo.



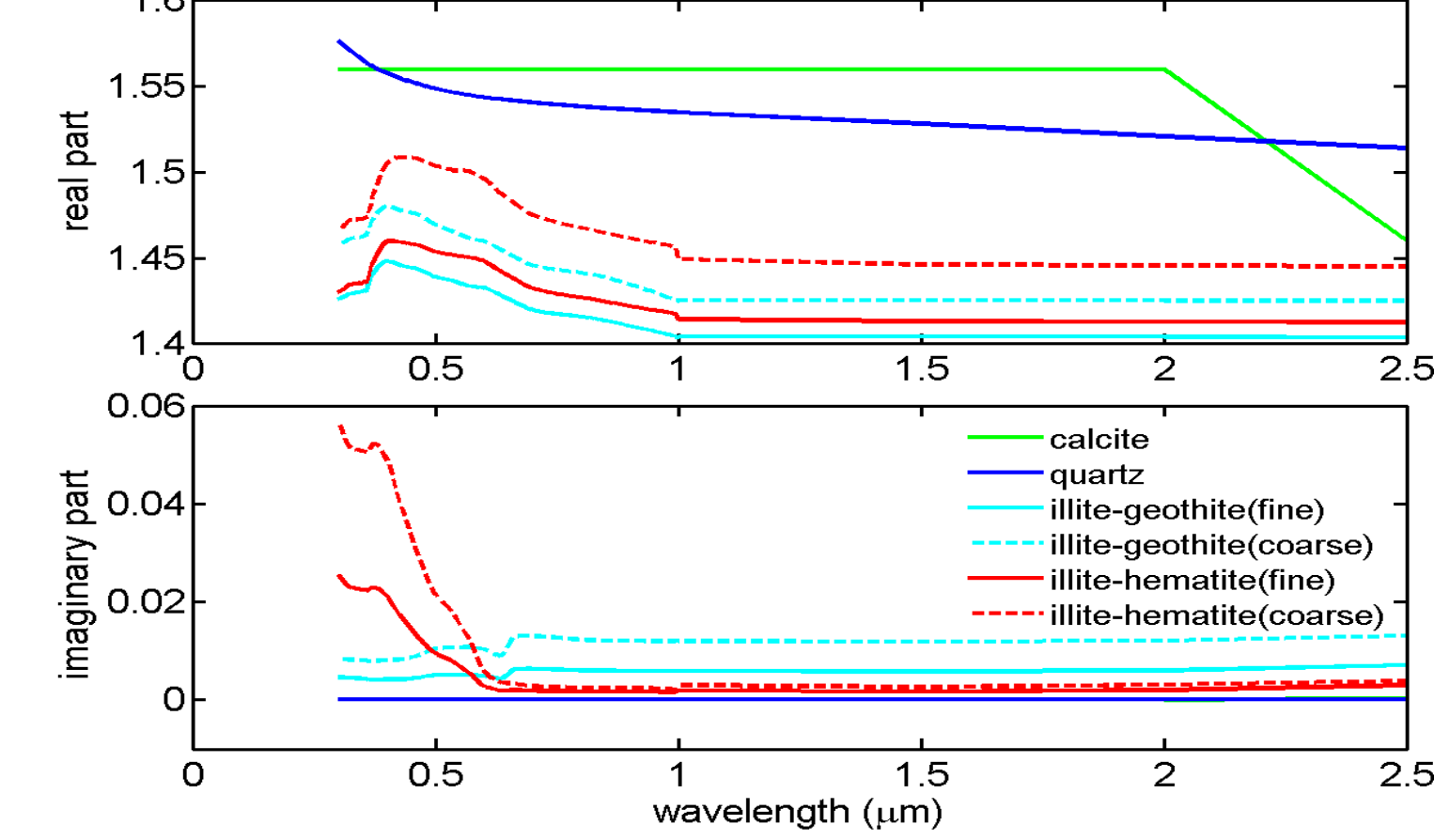
## 2. Data and Methodology



### 2.1 Computation of dust spectral optical properties

- The size-resolved mineralogical composition of Asian dust is represented by a mixture of individual minerals and iron oxide-clay aggregates based on recent measurements (Lafon et al. 2006). For each considered species, we use the spectral refractive indices from the UV to the thermal IR that enables a consistent representation of the dust optical properties over the entire range of wavelengths.

Refractive indices of individual minerals/aggregates:

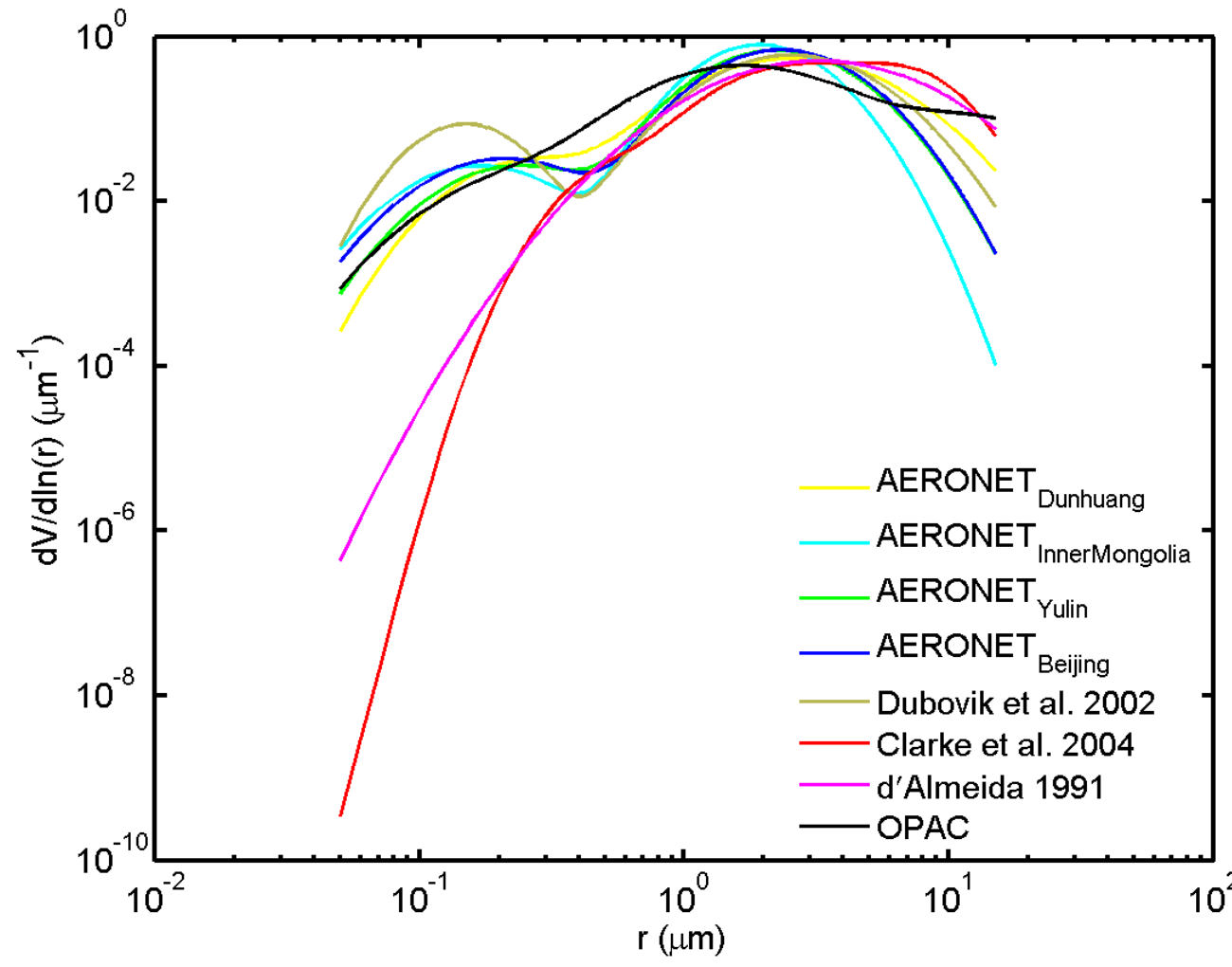


	Fine mode	Coarse mode
calcite	25%	29%
quartz	16%	28%
illite-geothite (IG)	59%*0.7	43%*0.7
illite-hematite (IH)	59%*0.3	43%*0.3

- To select the representative size distributions for dust aerosol, we examined the AERONET data (2001) at 4 Asian sites to identify dusty days with high  $\tau_{0.5}$  and low Angstrom exponent. Four size distributions from past studies are also used.

Size distribution	Reference	Fine mode (s)	Coarse mode
AERONET <sub>Dunhuang</sub>	Apr. 21 $\tau_{0.5}=1.31$ ANG=0.01	0.254 μm 1.697 μm 4.0%	2.561 μm 2.024 μm 96.0%
AERONET <sub>InnerMongolia</sub>	Apr. 30 $\tau_{0.5}=1.15$ ANG=0.01	0.169 μm 1.793 μm 3.6%	1.932 μm 1.623 μm 96.2%
AERONET <sub>Yulin</sub>	May 2 $\tau_{0.5}=1.26$ ANG=0.06	0.235 μm 1.738 μm 3.9%	2.23 μm 1.758 μm 96.1%
AERONET <sub>Beijing</sub>	May 1 $\tau_{0.5}=2.87$ ANG=0.23	0.209 μm 1.815 μm 4.9%	2.331 μm 1.738 μm 95.1%
B02	Dubovik et al., 2002	0.149 μm 1.52 μm 9.1%	2.538 μm 1.84 μm 90.9%
C04	Clarke et al., 2004	0.53 μm 1.48 μm 1.8%	2.751 μm 1.85 μm 69.4%
L91	d'Almeida, 1991	3.228 μm 100%	7.099 μm 20.5%
OPAC	Hess et al., 1998	0.267 μm 1.48 μm 3.4%	1.648 μm 2.0 μm 76.1%

Representative dust size distributions:



Dust (a) extinction coefficient (at 500 μm<sup>-1</sup>) and (b) single scattering albedo in the SW:

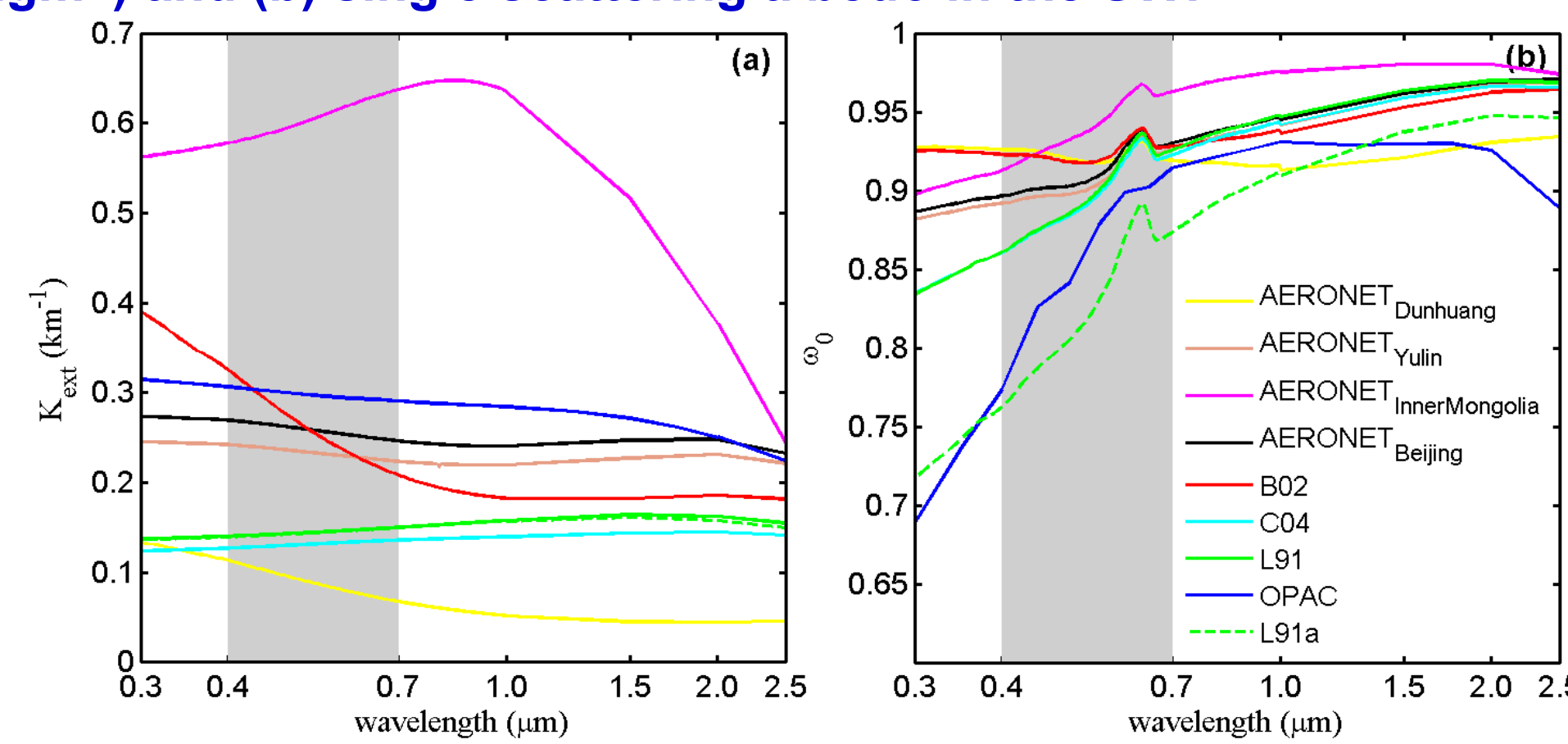
For the  $i$ -th mineral in  $j$ -th size mode, the normalized extinction coef. ( $\text{km}^{-1}/\text{cm}^{-3}$ ) is

$$K_{ext,j}^*(\lambda) = \sum f_{i,j} K_{ext,i,j}^*(\lambda)$$

The extinction coef. ( $\text{km}^{-1}$ ) is weighted by the number concentration of  $j$ -th mode ( $N_j$ ), calculated from the mass concentration and mass fraction:

$$K_{ext}(\lambda) = \sum N_j K_{ext,j}^*(\lambda)$$

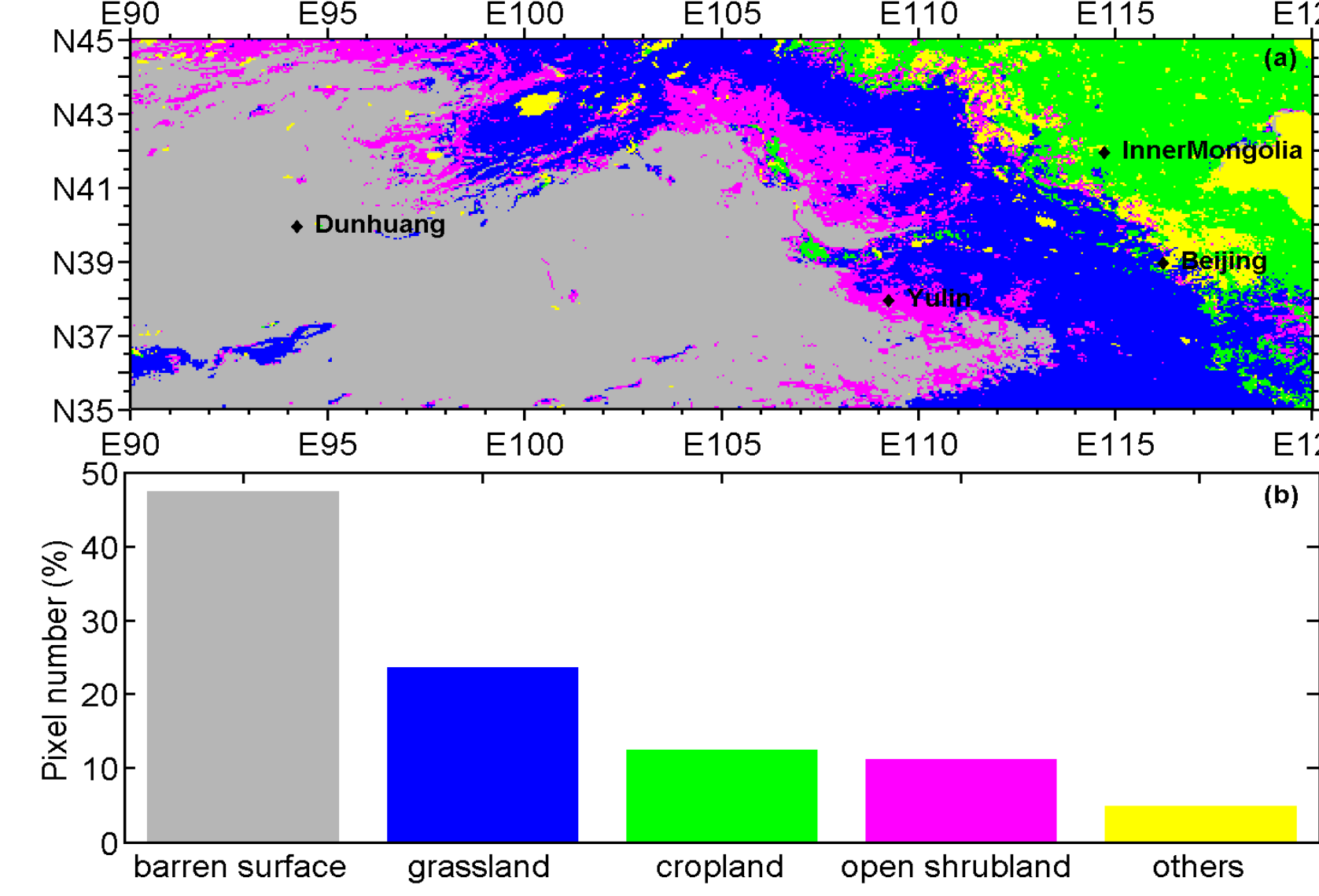
Single scattering albedo:

$$\omega_0(\lambda) = K_{sca}(\lambda) / K_{ext}(\lambda)$$


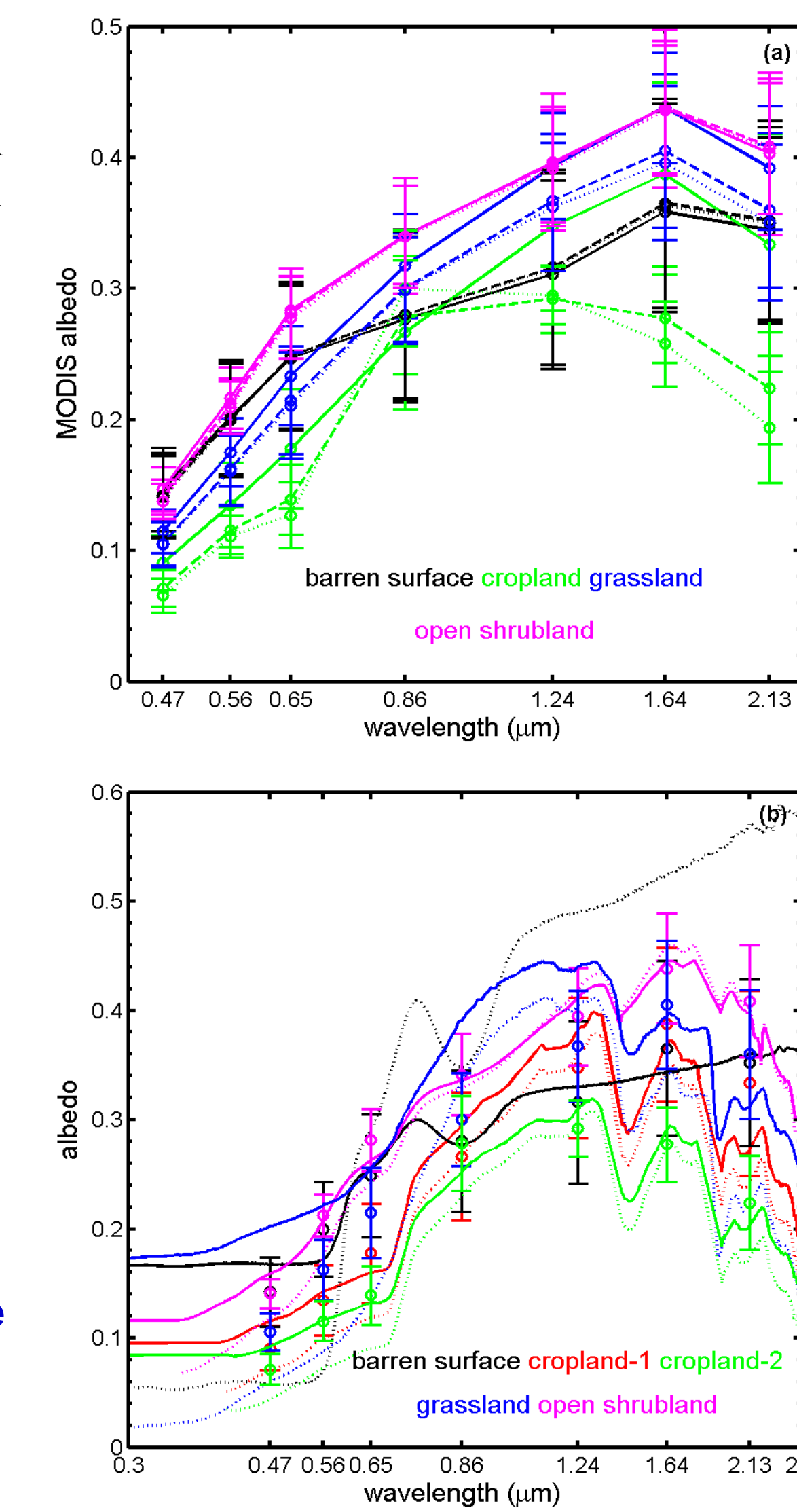
## 2.2 Spectral surface albedo of dryland ecosystems in East Asia

To obtain the spectral surface albedo for the different dryland ecosystems in East Asia, we used the MODIS climate modeling grid albedo product (MCD43C). The MODIS white-sky albedo at seven narrowbands was merged with the USGS spectral library to construct the detailed spectral albedo for different ecosystems (represented by MODIS land types).

Land cover map of the study region



(a) MODIS narrowband albedo for different dryland ecosystems, averaged for Apr. 23 (solid line), May 1 (dash line) and May 9 (dotted line) in 2001. (b) MODIS narrowband albedo (unfilled circle with error bar) is fitted using USGS dataset (dotted line) to construct the spectral surface albedo (solid line):



## 3. Results

### 3.1 Dust impact on surface PAR: modeled and observed

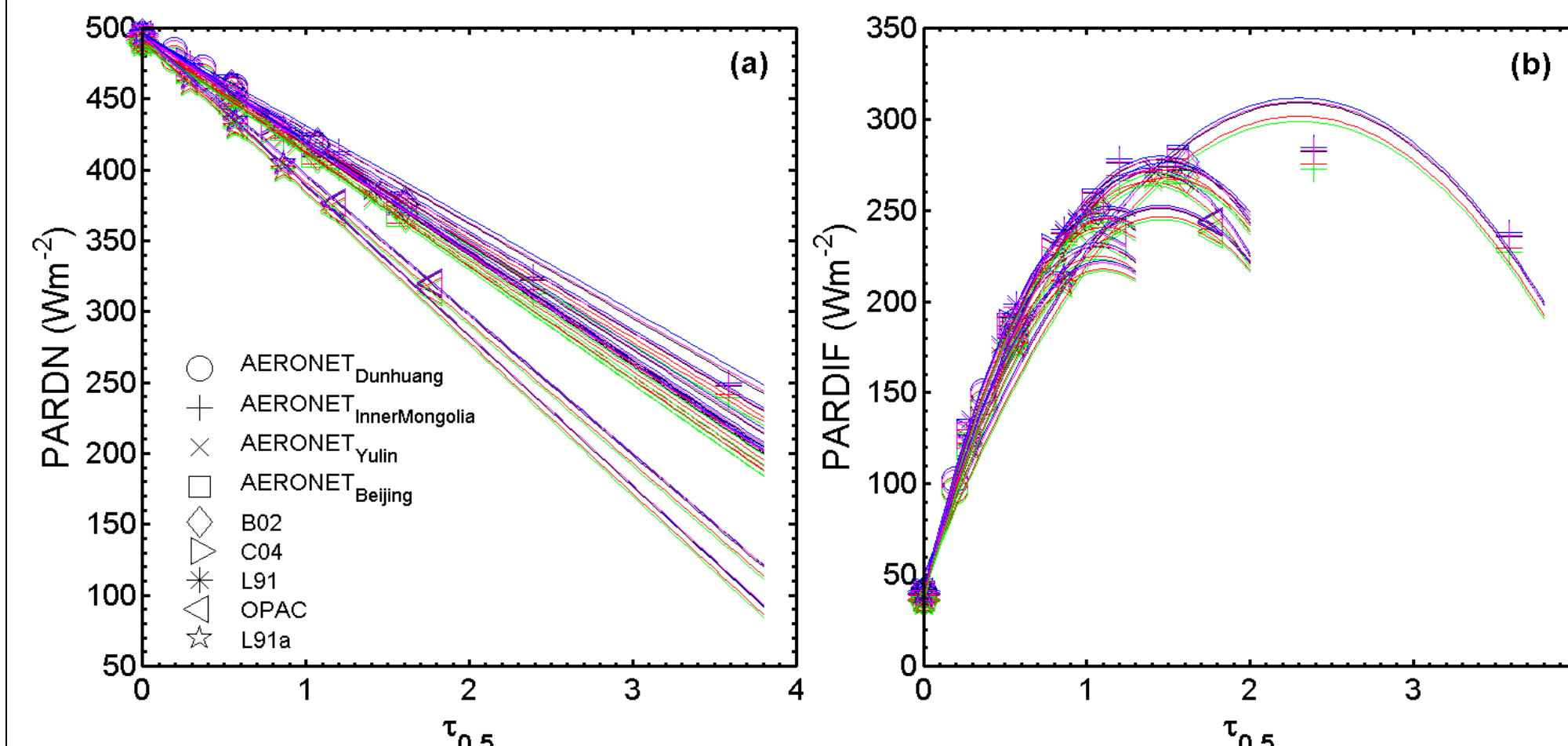
Different combinations of dust models and dryland ecosystems are fed to a radiative transfer code (SBDART) to compute surface spectral radiative fluxes, integrated over different wavelengths (SW, LW and PAR). Three dust loadings are considered: 250, 500 and 750 μg m<sup>-3</sup>. Dust profiles were constrained by using CALIPSO lidar observations: (1) mixed-layer 0–4 km case and (2) elevated-layer 5–9 km (results not shown).

Diffuse PAR: PARDIF=PARDN –PARDIR

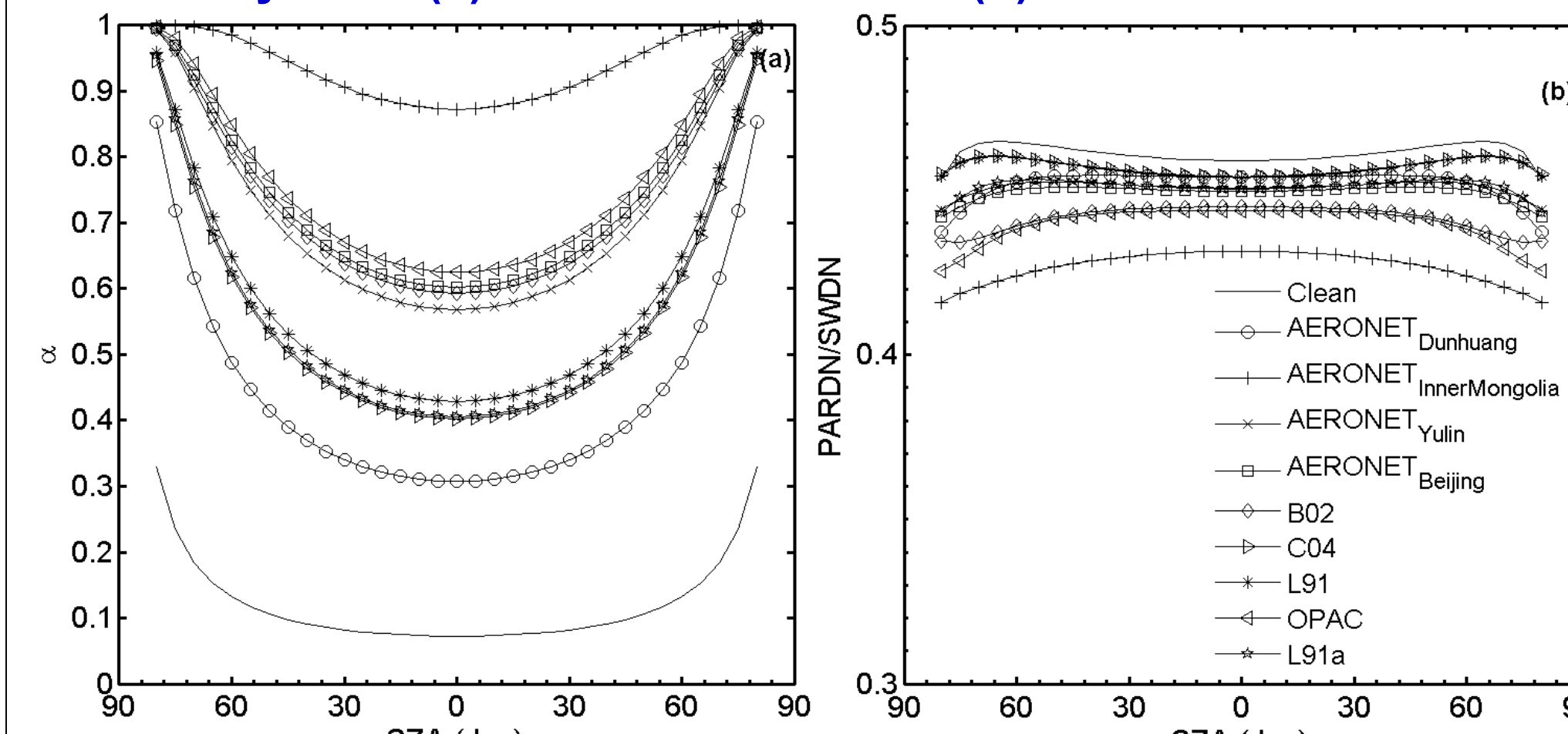
Diffuse fraction:  $\alpha = \text{PARDIF} / \text{PARDN}$

Forcing efficiency for PARDN:  $\delta_{\text{PARDN}} = \frac{d\text{PARDN}}{d\tau_{0.5}}$

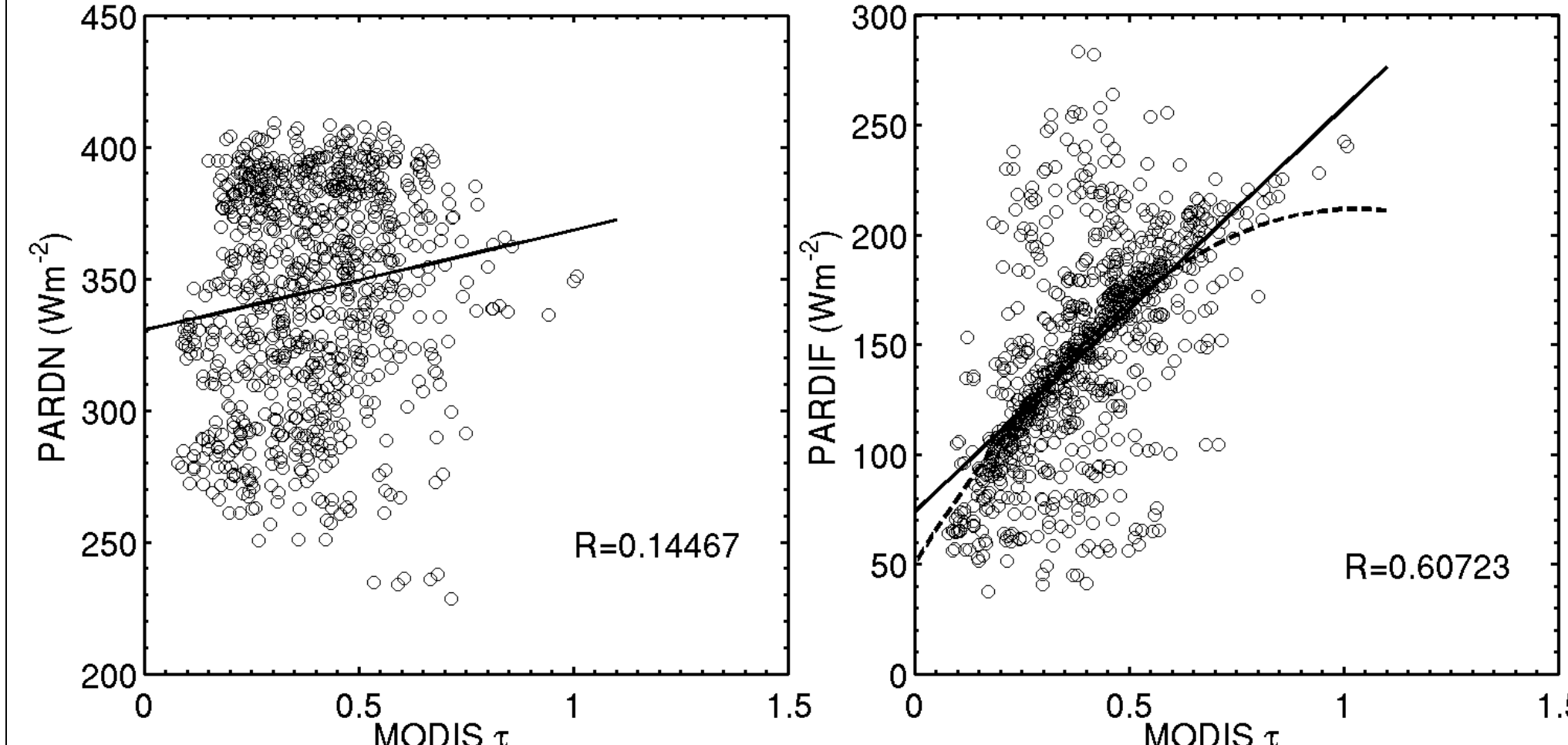
Changes in (a) surface downward and (b) diffuse PAR with dust optical depth:



Diurnal cycle of (a) diffuse fraction and (b) PARDN/SWDN:



Collocated (a) PARDN and (b) PARDIF with MODIS AOD:



- For a certain loading (mass), different dust models differ significantly in spectral Kext (and hence optical depth) and  $\omega_0$ , resulting in significant differences in the dust impact on PARDN and PARDIF.
- PARDIF shows that there is the optimal light environment for plant growth for each dust model at a certain dust optical depth.
- Slope of fitting lines equals  $\delta_{\text{PARDN}}$ , which mainly depends on  $\omega_0$  and to a lesser extent on surface albedo.

- $\alpha$  is higher at low SZA, but PARDN peaks at local noon. There would be a time period when the plant photosynthesis reaches its maximum due to the optimum levels of PARDN and  $\alpha$ .
- The diurnal cycle of PARDN along with the change in aerosol condition (assumed unchanged here) determines the diurnal behavior of the ecosystem production.
- PARDN/SWDN displays weak diurnal change (within 2%). At local noon, PARDN/SWDN is between 43.1% and 45.5%, lower than reported in Frouin and Pinker (1995)

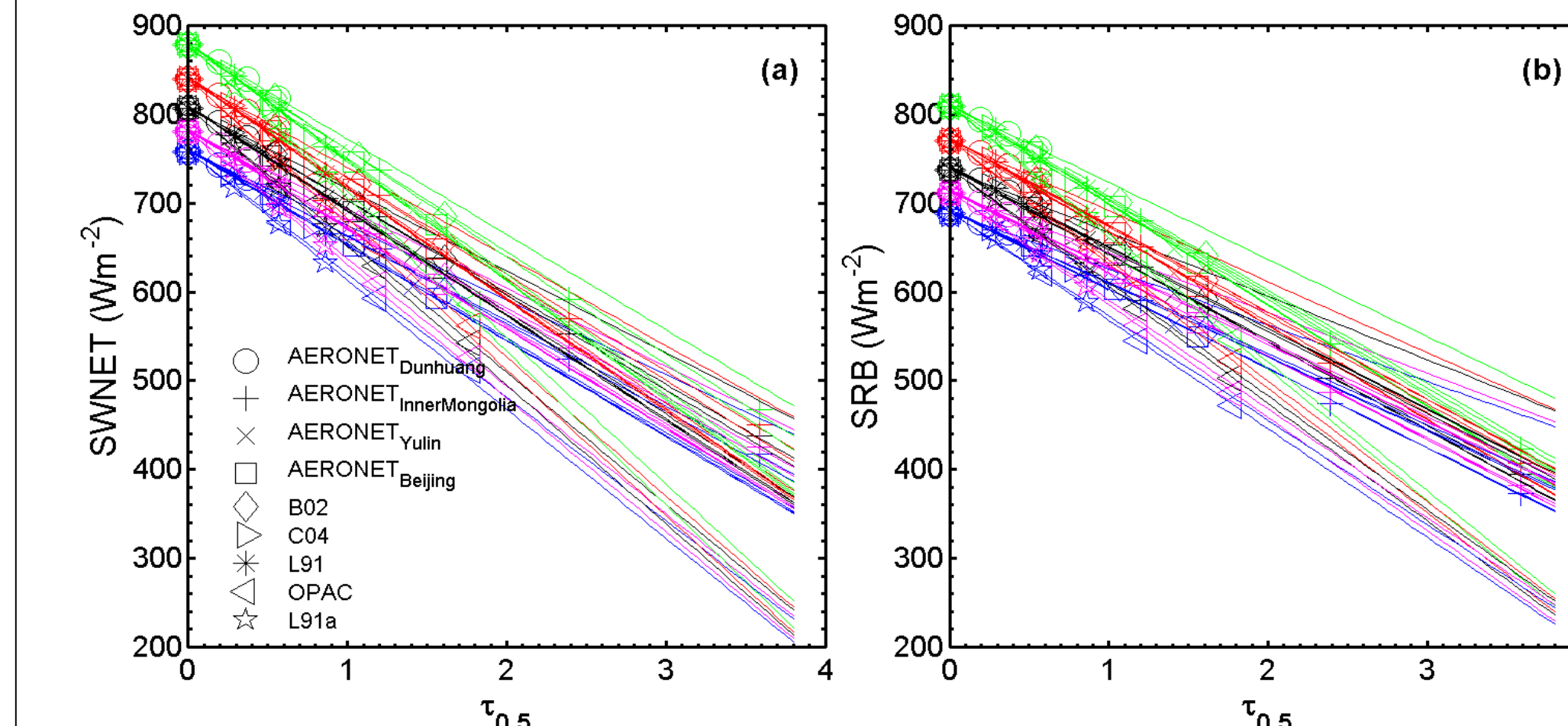
- PARDN and PARDIF are from CERES/Terra (FM1&FM2) SYN product (3hr averaged, 1-by-1 degree) for all the dryland ecosystems in the study region during 2001 spring.
- PARDN shows high variability and poor correlation with MODIS AOD, while PARDIF tends to increase linearly with increasing AOD.

## 3.2 Dust impact on surface radiative balance: modeled and observed

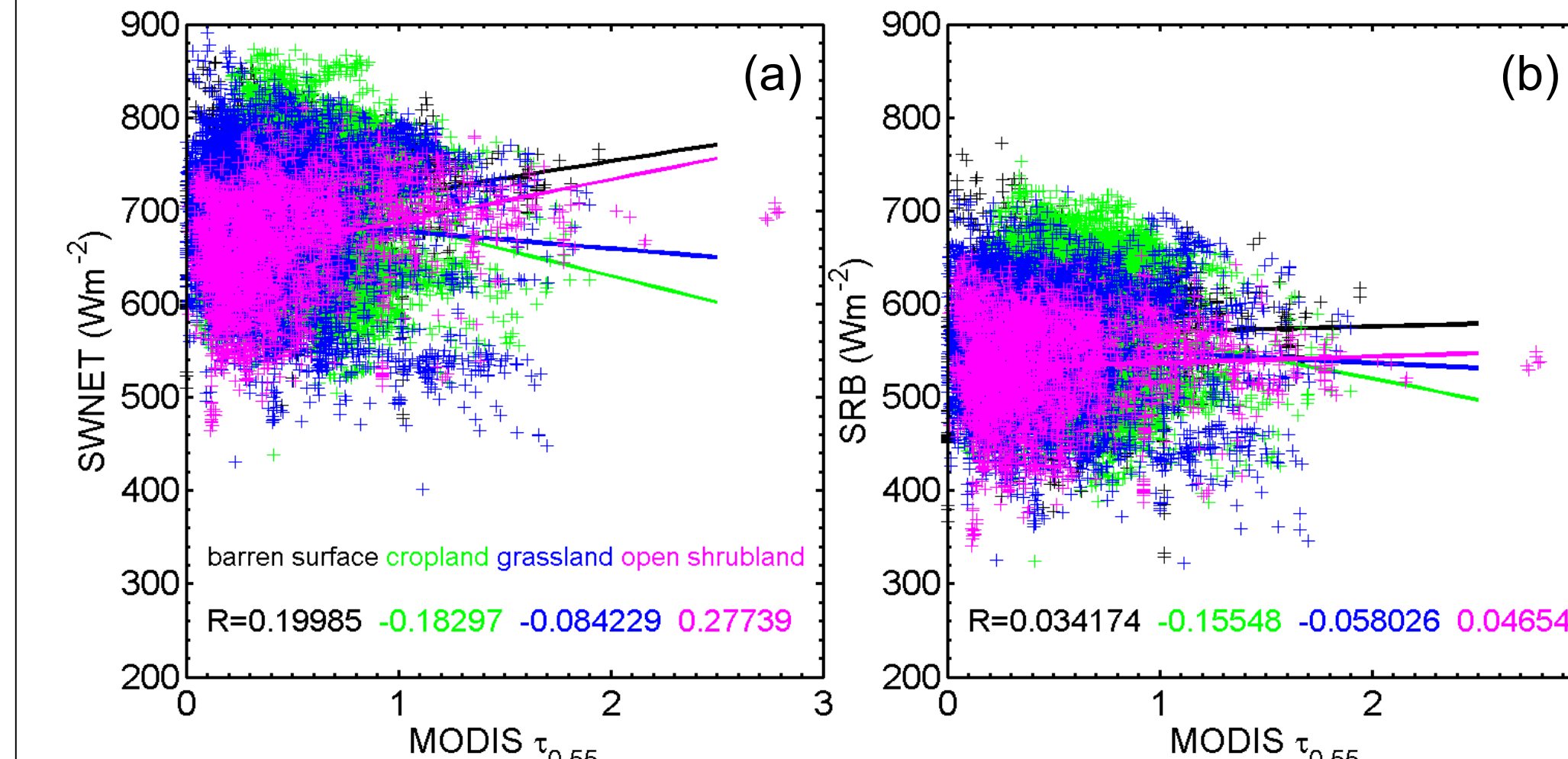
$$\text{SRB} = \text{SWNET} - \text{LWNET} = \text{SWDN} - \text{SWUP} + \text{LWDN} - \text{LWUP}$$

$$\text{Forcing efficiency for SWNET: } \delta_{\text{SWNET}} = \frac{d\text{SWNET}}{d\tau_{0.5}}$$

Changes in (a) surface SW net radiation and (b) surface radiative balance with AOD:



Collocated (a) SWNET and (b) SRB with MODIS AOD:



- Similar to PARDN, different dust models and ecosystems generate substantial difference in SWNET and SRB.
- $\delta_{\text{SWNET}}$  differs in magnitude from  $\delta_{\text{PARDN}}$  due to the spectral dependence of  $\omega_0$  in SW versus PAR.
- The dust positive LW effect compensates 6.1% – 34.4% of the SW reduction depending on the dust model, loading, and ecosystem surface albedo.

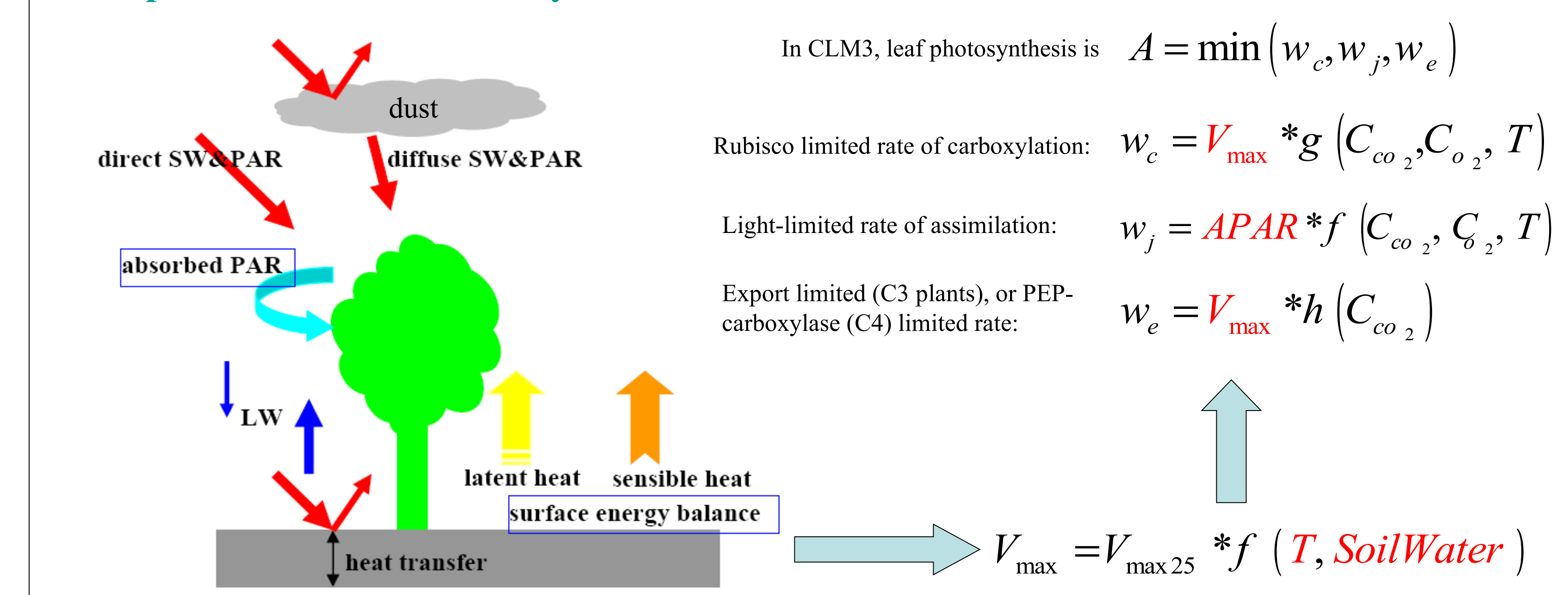
- SWNET and SRB are from CERES/Terra (FM1&FM2) SSF product Edition2B (hourly) for the study region during 2001 spring.
- Both SWNET and SRB reveal large variations. The LW warming compensates up to 55.2% of the SW reduction.
- Both SWNET and SRB show statistically insignificant correlations with MODIS AOD, pointing to the roles of various factors that need to be separated out.

## 4. Summary

### 4.1 Findings

- The size distributions considered cause significant differences in both the magnitude (by up to an order) and spectral behavior of the dust optical properties that result in a wide range of the impact on the surface PAR (amount and partitioning), SW, LW radiation and radiative balance.
- PARDN is reduced by 39–171 Wm<sup>-2</sup> over the cropland when dust loading=500 μg m<sup>-3</sup>.  $\delta_{\text{PARDN}}$  ranges -65.2– -106 Wm<sup>-2</sup>τ<sub>0.5</sub><sup>-1</sup> depending on the dust  $\omega_0$ . PARDIF increases with dust  $\tau$  and  $\omega_0$ , creating a favorable light environment for plant photosynthesis. The surface radiative balance is also reduced. This may affect the micrometeorology (temperature and humidity, etc) and the plant functioning.
- Our Asian dust models considering size-resolved composition exhibit very different optical and radiative properties from the bulk dust model from OPAC, showing the importance of accounting for region-specific dust size dynamics and composition in assessing the dust radiative impacts.
- CERES observations reveal poor agreement with the modeled dust impact on PAR and surface radiative balance, except for the diffuse PAR. Future work is needed to deep examine the multi-sensor observations.

### 4.2 Implication to aerosol-ecosystem interaction studies



## References

Lafon, S., I. N. Sokolik, J. L. Rajot, S. Caquineau, and A. Gaudichet (2006), Characterization of iron oxides in mineral dust aerosols: Implications for light absorption, *J. Geophys. Res.*, 111, D21207, doi:10.1029/2005JD007016.

Mercado L. M., N. Bellouin, S. Sitch, O. Boucher, C. Huntingford, M. Wild and P. M. Cox, Impact of changes of diffuse radiation on the global land carbon sink, *Nature*, 458, 1014–1017.

Oleson, K. W., et al. (2004), *Technical Description of the Community Land Model (CLM)*, NCAR Tech. Note NCAR/TN-461+STR, 174 pp., Natl. Cent. for Atmos. Res., Boulder, Colo.

Ricchiazzi, P., S. Yang, C. Gautier, and D. Sowle, 1998: SBDART: A Research and Teaching Software Tool for Plane-Parallel Radiative Transfer in the Earth's Atmosphere. *Bull. Amer. Meteor. Soc.*, 79, 2101–2114.

Sokolik, I. N., and O. B. Toon (1999), Incorporation of mineralogical composition into models of the radiative properties of mineral aerosol from UV to IR wavelengths, *J. Geophys. Res.*, 104(D8), 9423–9444.

Xi, X. and Sokolik, I. N., Impact of Asian dust aerosol and spectral surface albedo on the photosynthetically active radiation and surface radiative balance in dryland ecosystems, submitted to *ACPD*.

### Acknowledgements:

This work was funded by the NASA LCLUC.